Automated Mode Recovery for Gyrotrons demonstrated at Wendelstein 7-X

F. Wilde [a,b], S. Marsen[a], T. Stange[a], D. Moseev[a], J. W. Oosterbeek[a], H. P. Laqua[a], R. C. Wolf[a], K. Avramidis[b], G. Gantenbein[b], I. Gr. Pagonakis[b], S. Illy[b], J. Jelonnek[b,c], M. K. Thumm[b,c], W7-X team[d]

[a] *Max Planck Institute for Plasmaphysics, Wendelsteinstrasse 1, DE-17491 Greifswald, Germany*
[b] *IHM, Karlsruhe Institute of Technology (KIT), D-76131 Karlsruhe, Germany*
[c] *IHE, Karlsruhe Institute of Technology (KIT), D-76131 Karlsruhe, Germany*
[d] *See author list of R. C. Wolf Nucl. Fusion 57 (2017) 102020*

Abstract

The reliability of gyrotron operation is significantly decreased approaching the individual maximum output power of the tube due to loss of the nominal operating mode. For the first time, this paper proposes an algorithm for an automated mode recovery (MORE) for gyrotrons exploiting the hysteretic gyrotron behaviour. The algorithm has been implemented in a field-programmable gate array (FPGA) controlling the acceleration voltage and is able to recover the nominal operating mode within ≤ 1 ms after a mode switch to the competing satellite mode. This allows the gyrotron to be operated closer to its stability limits with extended pulse lengths at potentially higher output power. Dedicated experiments to test MORE were conducted at Wendelstein 7-X (W7-X) with two gyrotrons using a beam dump. The nominal mode could be successfully recovered in 99 % of 3755 modeloss events during 128 shots up to 20 s. MORE was operational for nine out of ten gyrotrons during the last experimental campaign OP1.2b of W7-X. The overall success rate during W7-X OP1.2b was 91 % counting 464 modeloss events in 131 shots performed with seven gyrotrons. Using the mode losses in the working point plane, the cutoff region for the nominal working mode was identified, defining a minimum cathode current for a given acceleration voltage. The total achievable output power of the W7-X ECRH plant could be increased by at least 500 kW for the same pulse length using MORE, assuming a conservative increase of at least 50 kW per gyrotron. Comparing the output power for the same achievable pulse length and reliability level, the output power increase per gyrotron is likely in the order of 100 kW. Since MORE exploits the hysteretic gyrotron behaviour, it could be applied to other gyrotrons of already existing or future ECRH facilities of fusion experiments, like ITER.

Keywords: gyrotron, mode recovery, satellite mode, hysteretic behaviour, field-programmable gate array

1. Introduction

Gyrotrons are commonly used in fusion research as high-power microwave sources for electron cyclotron resonance heating (ECRH) and electron cyclotron current drive (ECCD). Wendelstein 7-X (W7-X) uses ECRH as primary heating method for plasma production. At present, ten 140 GHz conventional cavity gyrotrons are available whereof eight are identical in construction [1]. Each gyrotron has a specified output power of 0.9 MW, operating on the $TE_{28,8}$-mode. Typically, the oversized cavity of a conventional, high-power gyrotron exhibits a dense mode spectrum, leading to strong mode competition (see [2, 3]). Approaching the maximum output power, satellite modes or other parasitic modes are easily excited simultaneously to the nominal operating mode. The quasi-optical output coupler converts these modes to stray radiation which cannot leave the gyrotron [4]. This results in a reduced efficiency, mostly in a mode loss, and potentially in a thermal damage. As a trade-off between operational stability and useable output power, the gyrotrons are therefore operated in a safe region at an empirically chosen working point below their maximum possible output power. At W7-X, a gyrotron is shutdown within 2 ms without RF (RF grace time) after a mode loss to prevent any damage. The affected gyrotron is then no longer available for the rest of the running plasma discharge and needs to be reset manually by an operator.

This paper presents an algorithm for an automated recovery of the nominal operating mode during a gyrotron pulse. Already existing approaches at DIII-D [5] or at ASDEX Upgrade (AUG) [6] shutdown the gyrotron and restart it after 10 (DIII-D) to 100 ms (AUG). Our approach does not shutdown the gyrotron but exploits the hysteretic gyrotron behaviour after a mode switch to the competing satellite mode. The nominal operating mode can be recovered this way within 200 μs (first attempt successful) up to the RF grace time of 2 ms (multiple attempts required to recover the mode).

*Corresponding author at: Max Planck Institute for Plasmaphysics, Wendelsteinstrasse 1, D-17491 Greifswald, Mecklenburg-Vorpommern, Germany. Tel: +49 3834 88 2528
Email address: fabian.wilde@ipp.mpg.de (F. Wilde)

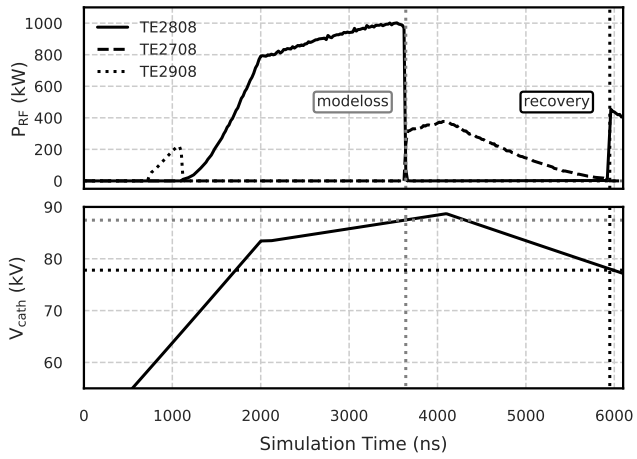

Figure 1: Exemplaric multi-mode simulation with EURIDICE [11] of the hysteretic gyrotron behaviour with respect to cathode voltage showing mode switching behaviour and subsequent mode recovery

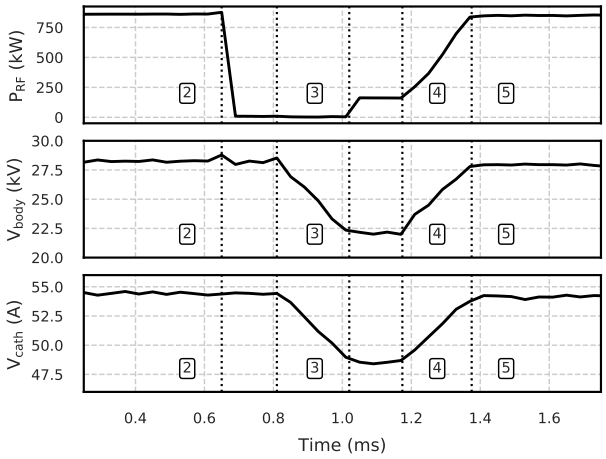

Figure 2: A mode recovery cycle during an experiment showing steps 2 to 5 of the algorithm. Waitstates in between are due to a time delay between the body and cathode voltage modulator.

2. Hysteretic Gyrotron Behavior

The hysteretic gyrotron behaviour has been examined in the past with respect to a variation of the acceleration voltage and magnetic field due to the mode competition in the oversized cavities (e.g. [7, 8]). The observations have in common that a mode switch could be quickly reversed by a reduction of the acceleration voltage. During experiments at W7-X, modeloss is often observed due to emitter cooling because of an inappropriate filament current boosting scheme or acceleration voltage noise when the gyrotron is operated close to the nominal working mode cutoff.

A simulation was performed with the multi-mode interaction code EURIDICE [1] using a set of 34 modes, including the gyrotron operating mode $TE_{28,8}$, its azimuthal neighbours (satellite modes) $TE_{27,8}$ and $TE_{29,8}$, and other parasitic modes which were identified in [9] for the W7-X gyrotrons. The code ARIADNE [10] was used to estimate electron beam parameters, voltage depression and calculate the magnetic field profile along the cavity for given main and gun field coil currents. Figure 1 shows that the gyrotron switches from the operating mode $TE_{28,8}$ to the lower satellite mode $TE_{27,8}$ during a voltage rampup at 87.5 kV. After the mode switch, the voltage is ramped down by 10 kV where the mode is recovered at 78 kV.

An experiment to examine the hysteretic behaviour with respect to the acceleration voltage was presented in [12]. A switch to the $TE_{27,8}$-mode was successfully provoqued and reversed with a sawtooth modulation of the acceleration voltage of at least 9 kV. A comparison between the simulation and the experiment shows a deviation of +3 % (9.65 kV vs. 9.91 kV) for the required voltage difference due to hysteresis to recover the nominal mode. This deviation could be explained by the acceleration voltage noise in the experiment.

3. Implementation

Each gyrotron has distinct power supplies for the cathode and the body voltage at W7-X [13]. The high-voltage power supplies (HVPS) allow a quasi real-time control of the acceleration voltage during the pulse. The MORE algorithm controls the acceleration voltage by temporarily overwriting the externally given set point values stored in a ring buffer. Both the cathode and the body voltage are controlled with a time delay where the sum of both has to equal the set point value for the acceleration voltage. A parameter is set to define how the acceleration voltage is shared between the cathode and the body voltage supply. In the following experiments, this parameter is set to 0.5. In [12] it is shown that the mode recovery is also successful when only the body voltage is modulated, but doing so would lead to an unnecessarily increased collector load. The pitch factor and the depression ratio are variable during MORE cycles and decreased by upto 10 % and 20 % respectively.

Based on the findings in [12], a mode recovery algorithm has been implemented using the already existing gyrotron controller based on a National Instruments cRIO-9039. This is an embedded system with a real-time operating system combined with a FPGA which can be programmed under the LabView environment. The mode recovery algorithm is implemented as a finite state machine as follows (see figure 2):

1. Wait for clearance (MORE is enabled, a pulse is running and the defined ignore period (typ. 20 to 100ms) is over). The ignore period is a time delay always applied at the beginning of the pulse after which MORE is allowed to be active.
   If clearance is given, go to step 2.
2. Wait for a mode loss (RF interlock state).
   If clearance is lost (since another interlock occurred

due to arcing, body current fault etc. or the pulse has ended), go back to step 1.
If a mode loss occurrs, save actual acceleration voltage $U_{ML,n}$. Check if this is the first mode loss during the pulse. If false,

- calculate the time distance Δt to the previous mode loss.
- check if $\Delta t \geq \theta$, where θ is a defined minimum time distance between two subsequent mode losses. If true, go to step 3, else go to step 6.

else go to step 3. This is a safety measure to avoid continous modulation which could reduce the lifespan of the gyrotron due to increased collector load. Otherwise the gyrotron duty cycle without emission would be unnecessarily increased.

3. Ramp down (RD) fast the acceleration voltage (within 200 μs) to the target voltage $U_{RD,n} = U_{RD,n-1} - \Delta_{RD}$ where $U_{RD,0}$ is the default target for the first attempt (during the pulse) to recover the mode (typ. 71 kV) and Δ_{RD} is a defined voltage step (typ. 0.2 kV). The ramp down target has a lower bound defined by the minimum acceleration voltage (typ. 68 kV). Then go to step 4.
If clearance is lost during the ramp down (e.g. RF grace time exceeded), go back to step 1.
4. Ramp up (RU) fast the acceleration voltage with a defined duration (typ. 200 μs) to $U_{RU,n} = U_{ML,n} - \Delta_{RU}$ with Δ_{RU} being a defined voltage step (typ. 0.1 to 1 kV). The minimum possible ramp up duration is limited by the slew rate of the high voltage power supply (here 4 μs/kV).
If the clearance is lost during the ramp up, go back to step 1.
If the mode was recovered (and is still active), go to step 5, else go to step 3.
5. Ramp up power slowly (PRU) either with
   (a) a constant defined slew rate SR_0 (typ. 20 to 100 ms/kV)
   (b) a variable slew rate $SR_n = SR_{n-1} + \Delta SR$ with $\Delta SR \approx 0.1 SR_0$

   after each consecutive mode loss during the pulse. The 2nd ramp up target value is
   (a) the momentary set-point value $U_{PRU,n} = U_{acc}(t_n)$, if the priority is maximum output power
   (b) $U_{PRU,n} = U_{ML,n} - \Delta_{PRU}$ where Δ_{PRU} is a voltage step, if the priority is operational stability. The acceleration voltage is then limited to $U_{PRU,n}$ to avoid any further mode loss events.

   If another mode loss occurrs during the power ramp up (PRU), go to step 2. If the 2nd ramp up is finished and the mode is still active, go to step 2.
6. Wait till the clearance is lost (which is the case when the RF grace time period is over or the shot has ended normally), then go to step 1.

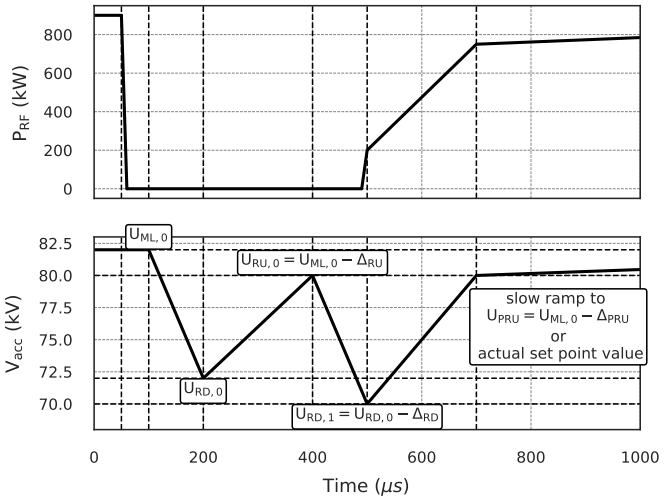

Figure 3: Illustration of a possible time trace for the RF output power and the acceleration voltage with two MORE attempts showing the algorithm variables

Figure 2 shows an exemplaric MORE cycle during an experiment. Due to a time delay between the body and cathode voltage modulator, a waiting period after the ramp down and ramp up is defined (typ. 20 μs).
The cathode current normally drops during the first seconds of the pulse, despite of using a boosting scheme for the filament heating current. The critical acceleration voltage U_{ML} where the mode is lost, was observed to follow the monotonically decreasing cathode current which stabilizes after a couple of seconds. This fact justifies step 5b of the algorithm. By adjusting the minimum allowed time distance θ between mode losses, the slew rate SR_0 for the 2nd ramp up and the voltage step Δ_{PRU}, the expected false-mode duty cycle can be controlled.
The aforementioned ignore period in step 1 of the algorithm is used so that MORE only becomes active during pulses exceeding a minimum duration. This is done for multiple reasons: First to guarantee that the neutralization is finished to support a successful mode recovery. Second to minimize the false mode duty cycle. Applying MORE for short pulses could lead to a high false mode duty cycle, assuming the minimum time period between subsequent mode losses to be set to a very small value. Finally MORE was intended to be used for longer and long pulses only.
Figure 3 shows the possible time traces of the RF output power and the acceleration voltage with two MORE attempts to illustrate the algorithm and its variables.

4. Results

A Python framework named SAGE (Statistical Analysis of Gyrotron Experiments) was developed to allow an automated evaluation and reduction of big amounts of gyrotron experiment data to a searchable database. The pre-

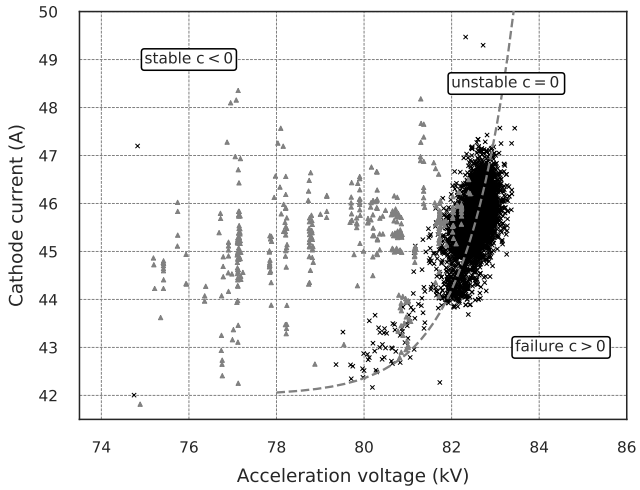

Figure 4: 3963 Modelosses (black crosses) and 425 stable shots (grey triangles) in the working point plane performed with the Alpha 1 (TED SN007) tube at nominal fields from dedicated MORE experiments and W7-X OP1.2b operation. The dashed line is a fit for the mode losses denoting a boundary between a stable and an unstable operation regime in the working point plane.

sented results are based upon the database using all gyrotron experiments performed during W7-X OP1.2b and dedicated test experiments with a beam dump. MORE was used with the maximum output power being set as priority.
The gyrotron shots are assigned to one of the following categories: stable (finished normally without MORE), unstable (finished normally with MORE), failed (ended prematurely despite the use of MORE).
In the following sections, the momentary RF output power is obtained with a power-calibrated detector diode signal where only the power of the nominal operating mode at 140 GHz is measured. The calibration is achieved by comparing the diode voltage signal to the integrated cooling water temperature difference in the beam dump, taking the transmission line losses into account to obtain the RF power at the gyrotron output window.

4.1. Operation regimes

Figure 4 shows 3963 modeloss events (black crosses) from 162 unstable and failed shots in the $(\mathrm{U_{acc}}, \mathrm{I_{cath}})$ working point plane. The average acceleration voltages and cathode currents for 425 stable shots (grey triangles) are shown as well. The shots with a duration of up to 55 s were acquired during dedicated MORE test experiments and W7-X OP1.2b operation for the Alpha 1 (TED SN007) tube at same (nominal) fields. The ratio between the body voltage $\mathrm{U_{body}}$ and the cathode voltage $\mathrm{U_{cath}}$, the depression ratio $\mathrm{U_{body}/U_{cath}}$, was held approximately constant at 0.51 across all shots with a maximum deviation of 4 % for 8 out of 162 shots.
The dashed curve fits the modelosses in the working point plane with the function

$$U_{max}(I) = \alpha_0 \ln(I + \alpha_1) + \alpha_2 \tag{1}$$

or alternatively

$$I_{min}(U) = \exp\left(\frac{U - \alpha_2}{\alpha_0}\right) - \alpha_1 \tag{2}$$

where $\alpha_0 = 1.1$, $\alpha_1 = -42$ and $\alpha_2 = 81.135$.
All stable shots are in the upper left area enclosed by the fit line. A possible conclusion is that the fit denotes the center of a cutoff region for the nominal operating mode where multi-moding and mode loss are more likely. For each acceleration voltage $\mathrm{U_{acc}}$ exists a minimum critical cathode current I_{min}. The width of this boundary region is reflected by the width of the mode loss point cloud. The noise of the measured acceleration voltage and cathode current surely contributes to the width of the boundary region, but should not be considered as the only explanation.

The existence of such a boundary region in the working point plane is supported by multiple findings: It is supported by satellite mode stray radiation measurements presented in [12], where the increased stray radiation level of the satellite modes near the output power limit is proposed as a modeloss precursor. Secondly, multi-moding of the nominal operating mode $\mathrm{TE_{28,8}}$ and its satellites $\mathrm{TE_{27,8}}$ and $\mathrm{TE_{29,8}}$ is observed in multi-mode simulations with EURIDICE [11] mimicking the emitter cooling behaviour with decreasing beam current as observed in experiments. The shape of the fit curve is also plausible: When the gyrotron is operated close to the boundary, a small change in voltage suffices to cause a mode switch. On the other hand, the boundary is slowly approached by a slowly decreasing cathode current, allowing (temporary) multi-moding behaviour to be observed.

Since the gyrotron failure probability depends on the targeted pulse length and the working point, a new quantity called criticality is proposed to denote the stability of gyrotron operation defined as

$$\mathrm{d} = \sqrt{(\mathrm{U} - \mathrm{U_0})^2 + (\mathrm{I_{min}(U)} - \mathrm{I_0})^2} \stackrel{!}{=} \min \tag{3}$$

$$\mathrm{p} = \mathrm{sgn}\left(\mathrm{U_{max}(I_0)} - \mathrm{U_0}\right) \cdot \mathrm{sgn}\left(\mathrm{I_{min}(U_0)} - \mathrm{I_0}\right) \tag{4}$$

$$\mathrm{c} = \mathrm{p} \cdot \mathrm{d} \tag{5}$$

where the criticality c is the minimum distance d from the actual working point $(\mathrm{U_0}, \mathrm{I_0})$ to the fit line $(\mathrm{U}, \mathrm{I_{min}(U)})$. The criticality is negative for a working point in the stable region and approaches and exceeds zero with increasing criticality.

4.2. Increase of Reliable Output Power

The automated mode recovery enables the gyrotron to be operated closer to its output power limit at more unstable working points near the cutoff. Consequently the maximum reliable output power could be increased for the

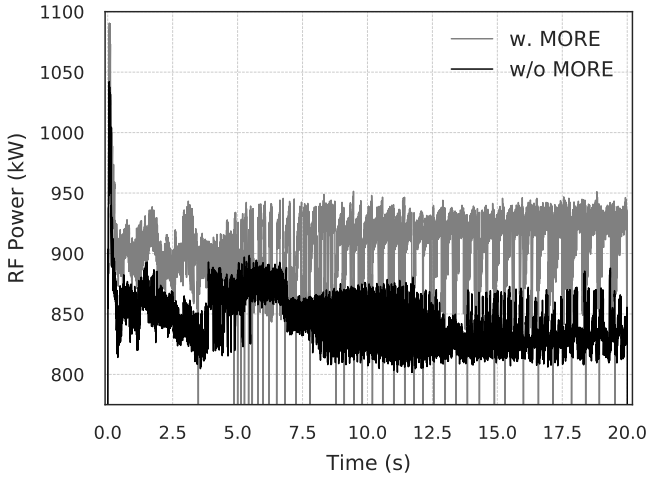

Figure 5: Comparison of maximum achievable output power with (grey) / without (black) MORE for the Alpha 1 (TED SN007) tube measured at the gyrotron output window

same pulse length. The averaged output power for a 20 s pulse with Alpha 1 could be increased by 7% from 859 kW to 916 kW for the fundamental gaussian mode at the output window. This is a conservative estimate based on the achieved integrated temperature difference in a water-cooled load, including therefore 3.5% transmission line loss and 1% reflection in the load. A comparison is given in figure 5. The average output power stabilizes and slightly increases towards the end of the shot. Therefore, the improvement for steady state operation is even higher, because the maximum momentary output power could be increased by up to 11 % around 100 kW. A similar result was achieved with Bravo 5 where an improvement by 5% at nominal and by 7% at alternative fields was observed using the conservative estimate. Note that these values do not take into account the reduced gyrotron reliability at this output power level and pulse length without MORE. Comparing the achievable output power with and without MORE with the same pulse length and reliability level, the increase of the reliable output power would be likely higher, but more data are required to support this statement.

4.3. Dedicated MORE Experiments

In total 178 shots with upto 20 s duration were performed to test the automated mode recovery in preparation for W7-X OP1.2b using the Alpha 1 (TED SN007) gyrotron at nominal fields. The overall success rate for the mode recovery is 99 % for 3755 mode loss events during 178 shots, whereof 50 were stable, 84 were unstable and 44 have failed.

In order to quantify the improvement in terms of operational reliability using MORE, the average achieved pulse length, the mean time to failure (MTTF) and the mean failure probability (MFP) were calculated. The MTTF and MFP were calculated for different criticality intervals representing working points with different distances to the cutoff line of the nominal working mode in the working point plane. The cutoff line of the nominal working mode is shown in Figure 4. Therefore the criticality was the independent variable in those cases. The average achieved pulse length was calculated for different RF output power intervals. Therefore the RF output power was the independent variable in that case. A simple approach for the MTTF is used with $\mathrm{MTTF} = (1/\mathrm{N_{failed}}) \sum \tau_\mathrm{i}$ where τ is the achieved pulse length and $\mathrm{N_{failed}}$ the number of failed shots for each interval of the independent variable. Furthermore the mean failure probability (MFP) is the ratio $\mathrm{N_{failed}}/\mathrm{N_{total}}$ with $\mathrm{N_{failed}}$ being the number of failed shots and $\mathrm{N_{total}}$ the number of total shots for each given interval of the independent variable. The achieved pulse length without MORE is defined as the pulse length till the first mode loss.

The overall average achieved pulse length across all output power intervals using MORE is 14.7 s in contrast to 4.9 s achieved without MORE. The overall achieved MTTF using MORE is 42.8 s in contrast to 12.7 s achieved without MORE. The average duration of MORE cycles during pulses is 532 μs. The available time for MORE attempts is limited by the maximum allowed time period without RF (RF grace time) which was set to 2 ms. The average false mode duty cycle is 9.6×10^{-4} and the average voltage modulation frequency is 2.2 kHz. According to [14], for a cyclic load with $f \geq 1$ kHz with low duty cycle, no significant effect on the collector lifespan is expected. The additional expected collector heat load due to MORE is therefore negligible and a significant reduction of the collector lifespan is unlikely.

Figure 6a shows that the effect of MORE on the achieved pulse length is stronger for higher output powers. The criticality c introduced in section 4.1 is a better independent variable than the output power since it incorporates the cathode current and the acceleration voltage. Figures 6c and 6d show a clear trend that the MTTF is decreasing and the MFP is increasing fast with increasing criticality similar to a cumulative Weibull distribution known from failure analysis in engineering. Figure 6d shows that MORE reduces the MFP significantly in particular close to the cutoff for criticality values near $c = 0$, hence towards higher output power. The MFP of the gyrotron when operated close to the cutoff or its output power limit is reduced by -27.3 % up to -77 % from 53.7 % to 12.2 %. The MTTF is increased by $+41.2$ % up to $+753.5$ % for high criticality values as shown in Figure 6c. Note that also stable shots were taken into account, deminishing the effect of MORE for low criticality values far from the cutoff line. Figure 6a shows that the average achieved pulse length is improved by $+123.4$ % up to $+246.4$ % from 3.32 s to 11.5 s. This indicates reliability improvements for pulses of all given RF output power intervals with a fixed target pulse length. All three quantities, the average achieved pulse length, the MTTF and the MFP indicate an improvement in terms of

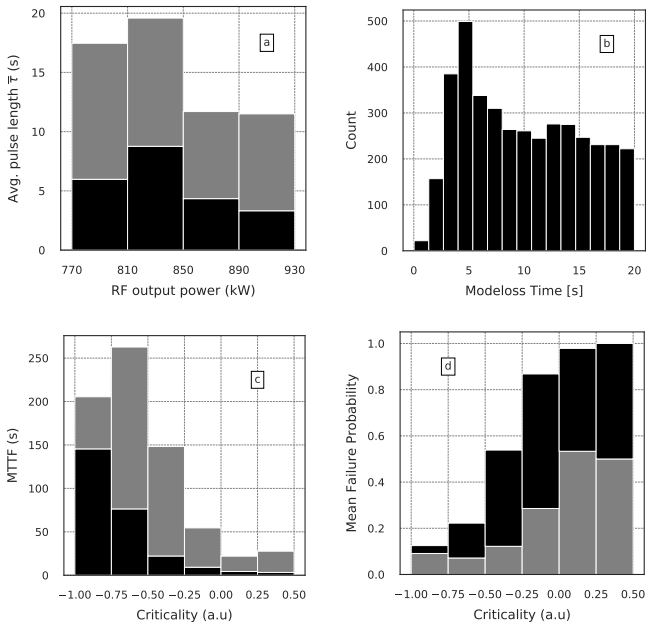

Figure 6: a) Average achieved pulse length for gyrotron output power intervals, b) histogram for modeloss times, c) MTTF for criticality intervals, d) MFP for criticality intervals with (grey) and without (black) MORE. Note that also stable shots were taken into account.

Name	SN	#	ML	MORE	Success [%]
Alpha 1	**7**	**65**	**331**	**308**	**93**
Alpha 5	5	6	15	13	87
Bravo 1	M	8	23	23	100
Bravo 5	2i	8	10	7	70
Charly 1	1	15	14	9	64
Delta 1	**6**	**25**	**66**	**58**	**87**
Delta 5	3	4	5	3	60
Total		**131**	**464**	**421**	**91**

Table 1: MORE results from W7-X OP1.2b operation: the number of mode losses (ML) compared with the number of successful mode recoveries (MORE) leads to a MORE success rate

Name	$\overline{\tau}$ [s]	$\overline{\tau}_{\mathbf{MORE}}$ [s]	$\boldsymbol{\Delta}$ [%]
Alpha 1	**3.10**	**4.61**	**49**
Alpha 5	4.54	6.66	47
Bravo 1	3.47	4.25	22
Bravo 5	3.26	4.45	36
Charly 1	3.56	3.76	6
Delta 1	**1.69**	**2.87**	**70**
Delta 5	3.07	3.11	1
Overall	**3.07**	**4.31**	**40**

Table 2: Comparison of average achieved pulse length without and with MORE during W7-X OP1.2b operation

gyrotron reliability close to its output power limit when MORE is used. Figure 6b presents a histogram at which time modelosses occurred during the pulses. Modelosses accumulated in the first 2 to 6 s of the pulses due to a cathode current dip in the course of the first fast, then slowly changing cathode current. Therefore modelosses are uniformly distributed later-on when the gyrotron is operated close to its limit.

4.4. Wendelstein OP1.2b - Operation

During W7-X OP1.2b from 18th July 2018 to 18th October 2018, 9813 shots with upto 100 s were performed. MORE was not fully operationable for nine out of ten gyrotrons before 25th August 2018, so only shots where MORE was enabled with a duration of at least 100 ms were taken into account. This lower limit for the duration was choosen since MORE was set to be active after 100 ms, leaving 8651 shots for 10 gyrotrons in total.

Increased ambient temperatures during the experiment campaign caused massive arcing in a part of the transmission line without sufficient air conditioning. High power shots were therefore hardly feasible during that campaign, so data with MORE cycles exist only for seven gyrotrons, mostly for Alpha 1 and Delta 1. Table 1 shows the MORE success rate during W7-X OP1.2b. Please note that the MORE parameters were thoroughly optimized for Alpha 1, Bravo 1 and Bravo 5 only and the sample size is much smaller for the other gyrotrons. The overall achieved MORE success rate for seven gyrotrons combined is 91%.
So far no parasitic effect, for example cross talk between gyrotrons operated simultaneously, has been observed using MORE.

5. Conclusion

We take advantage of the already existing control sytem and the RF power measurement, so that there were no additional costs for the implementation of MORE at W7-X. When the costs for the necessary hardware are taken into account, this solution still offers a very attractive cost-benefit-ratio (approximately 1:7) comparing the solution costs to the worth of the achieved increase in terms of reliable output power. In this case 100 kW of gyrotron output power are estimated to 100.000 euros.
The total reliable output power of the W7-X ECRH plant could be increased by at least 500 kW for the same pulse length, assuming a conservative increase of at least 50 kW per gyrotron. As shown in section 4.2, the increase of reliable output power is more likely in the order of 100 kW, compared to the highest achievable output power without MORE. The decreased gyrotron reliability at that output power level without MORE is neglected in that case.
Improving the acceleration voltage quality, hence reducing the noise (e.g ripple and overshoot), and a better emitter temperature control would have a big impact on the gyrotron working point stability in particular close to the cutoff of the working mode. Under the given constraints that no technical modification of the gyrotron or its power supplies were possible, MORE seemed to be the most suitable solution.

Since the algorithm exploits the hysteretic gyrotron behaviour, it could be also applied to any other gyrotron using a high-voltage power supply meeting the required modulation capabilities. Therefore the presented findings are also significant for other already existing and future ECRH facilities of fusion experiments, like ITER.

Acknowledgements

This work has been carried out within the framework of the EUROfusion Consortium and has received funding from the Euratom research and training programme 2014-2018 and 2019-2020 under grant agreement No 633053. The views and opinions expressed herein do not necessarily reflect those of the European Commission.

References

[1] V. Erckmann, P. Brand, H. Braune, G. Dammertz, G. Gantenbein, W. Kasparek, H. P. Laqua, H. Maassberg, N. B. Marushchenko, G. Michel, M. K. Thumm, Y. Tuzrkin, M. Weissgerber, A. Weller, W.-X. E. T. at IPP Greifswald, W.-X. E. T. at FZK Karlsruhe, W.-X. E. T. at IPF Stuttgart, Electron Cyclotron Heating for W7-X: Physics and Technology, Fusion Science and Technologydoi:10.13182/FST07-A1508.

[2] M. V. Kartikeyan, E. Borie, M. K. A. Thumm, Gyrotrons - High-Power Microwave and Millimeter Wave Technology, Vol. 1, Springer, 2004.

[3] G. S. Nusinovich, Introduction to the Physics of Gyrotrons, Vol. 1, The John Hopkins University Press, 2004.

[4] M. Thumm, X. Yang, A. Arnold, G. Dammertz, G. Michel, J. Pretterebner, D. Wagner, A High-Efficiency Quasi-Optical Mode Converter for a 140-GHz 1-MW CW Gyrotron, IEEE Transactions on Electron Devices 52 (5) (2005) 818–823. doi:10.1109/TED.2005.845791.

[5] D. Ponce, R. Brambila, M. Cengher, Y. Gorelov, W. Grosnickle, J. Lohr, A. Torrezan, Interrupting an Imminent Body Current Fault and Restoring Full Power in Milliseconds on a DIII-D National Fusion Facility Gyrotron, Fusion Science and Technology 73 (1-4). doi:10.1080/15361055.2017.1387009.

[6] D. Wagner, J. Stober, F. Leuterer, F. Monaco, S. Müller, M. Münich, C. J. Rapson, M. Reich, M. Schubert, H. Schütz, W. Treutterer, H. Zohm, M. Thumm, T. Scherer, A. Meier, G. Gantenbein, J. Jelonnek, W. Kasparek, C. Lechte, B. Plaum, T. Goodman, A. G. Litvak, G. G. Denisov, A. Chirkov, V. Zapevalov, V. Malygin, L. G. Popov, V. O. Nichiporenko, V. E. Myasnikov, E. M. Tai, E. A. Solyanova, S. A. Malygin, ASDEX Upgrade Team, Status, Operation, and Extension of the ECRH System at ASDEX Upgrade , Journal of Infrared, Millimeter, and Terahertz Waves 37 (1) (2016) 45–54. doi:10.1007/s10762-015-0187-z.

[7] O. Dumbrajs, T. Idehara, Hysteresis in Mode Competition in High Power 170 GHz Gyrotron for ITER, International Journal of Infrared and Millimeter Waves 29 (3) (2008) 232–239. doi:10.1007/s10762-008-9325-1.

[8] O. Dumbrajs, T. Idehara, Y. Iwata, S. Mitsudo, I. Ogawa, B. Piosczyk, Hysteresis-like effects in Gyrotron Oscillators, Physics of Plasmas 10 (5) (2003) 1183 – 1186. doi:10.1063/1.1561277.

[9] A. Schlaich, Time-dependent spectrum analysis of high power gyrotrons, Ph.D. thesis, KIT (2014). doi:10.5445/KSP/1000046919.

[10] I. G. Pagonakis, J. Vomvoridis, The self-consistent 3D trajectory electrostatic code ARIADNE for gyrotron beam tunnel simulation, 9th Int. Conf. Infr. Millim. Waves, 12th Int. Conf. Terahertz Electron. Conf. Dig. (2004) 657–658doi:10.1109/ICIMW.2004.1422262.

[11] K. A. Avramidis, I. G. Pagonakis, C. T. Iatrou, J. L. Vomvoridis, EURIDICE: A code-package for gyrotron interaction simulations and cavity design, EPJ Web of Conferences 32 (04016). doi:10.1051/epjconf/20123204016.

[12] F. Wilde, H. P. Laqua, S. Marsen, T. Stange, K. A. Avramidis, G. Gantenbein, J. Jelonnek, S. Illy, I. G. Pagonakis, M. Thumm, Measurements of Satellite Modes in 140 GHz Wendelstein 7-X Gyrotrons: An Approach to an Electronic Stability Control, 2017 Eighteenth International Vacuum Electronics Conference (IVEC) (2017) 1–2doi:10.1109/IVEC.2017.8289661.

[13] H. Braune, P. Brand, R. Krampitz, W. Leonhardt, D. Mellein, G. Michel, G. Mueller, J. Sachtleben, M. Winkler, the W7-X ECRH teams at IPP IPF, FZK, HV-system for CW-gyrotrons at w7-x and the relevance for ITER, Journal of Physics: Conference Series 25 (2005) 56–65. doi:10.1088/1742-6596/25/1/008. URL https://doi.org/10.1088%2F1742-6596%2F25%2F1%2F008

[14] V. E. Miasnikov, V. O. Nichiporenko, L. G. Popov, S. V. Usachev, Y. M. Yashnov, Endurance of the highly heat-stressed units exposed to cycling loading in 1MW/170 GHz CW gyrotron for ITER, IRMMW-THzdoi:10.1109/IRMMW-THz.2016.7758514.